Reevaluating Lunar Laser Ranging, Type 1A Supernovae, and Earth Thermal History Constraints on Epoch-Dependent G Models

Marco Pereira
Email: ny229200@gmail.com

Abstract:
This paper critically reexamines the constraints on the variability of Newton's gravitational constant, G, imposed by three primary lines of reasoning: (1) Earth's thermal history and the Young Faint Sun Paradox, (2) Type Ia Supernova (SN1a) luminosity constraints, and (3) Lunar Laser Ranging (LLR) data used to model Earth's rotational slowdown. Conventional analyses assume a constant G over cosmological timescales, leading to potentially flawed constraints. We demonstrate that these constraints fail to incorporate key epoch-dependent considerations, and when properly accounted for, variations in G remain within observational uncertainty.

The Young Faint Sun Paradox is resolved by incorporating continuous hydrogen accretion by the Sun over 4.5 billion years, which stabilizes Earth's temperature without requiring a constant G. SN1a constraints are reassessed by explicitly deriving the G-dependence of SN1a's Absolute Luminosity using David Arnett's modeling of supernova detonation physics. We show that current SN1a photometric distance estimates are systematically biased under the assumption of a constant G. The LLR-based constraints fail because NASA's analysis does not derive epoch-dependent G corrections for the conservation of total angular momentum. A full-fledged epoch-dependent G model demonstrates that variations in G would affect Earth's Moment of Inertia dynamics below 0.2%, within observational precision.

We introduce the **Hypergeometrical Universe (HU) model to support these findings**, which postulates that the universe expands as a lightspeed-expanding hyperspherical hypersurface. HU predicts an epoch-dependent G and redefines matter as composed of polymers of **Fundamental Dilators (FDs)**, metric wave generators that interact via the dilaton field. The **Quantum Lagrangian Principle (QLP)** further enforces a "no work" condition for particle motion in the 4D spatial manifold. HU replaces the standard Big Bang paradigm with the **Big Pop Cosmogenesis**, which resolves key cosmological inconsistencies without inflation, dark matter, or dark energy.

We provide explicit derivations of the SN1a absolute luminosity dependence on G, demonstrate that observed cosmic acceleration may be an artifact of improper calibration rather than dark energy, and argue that LLR constraints on G-variability are overstated. Additionally, we show that a stronger G in early epochs explains the Great Attractor's velocity field and early galaxy formation. We conclude that a proper epoch-dependent treatment of gravitational physics is necessary to reassess G's evolution over cosmic time, fundamentally altering our understanding of cosmology and planetary dynamics.

1. Introduction

Newton's gravitational constant, G, is one of the fundamental parameters of physics, but its constancy over cosmological time remains an open question. Observational constraints on G-variability are indirect, often relying on assumptions embedded in astrophysical and geophysical models. Three widely cited constraints arise from:

1. The Young Faint Sun Paradox suggests that a weaker Sun in the past should have led to a frozen Earth, which conflicts with geological evidence of liquid water and early life.
2. Type Ia Supernovae (SN1a) as standard candles, which assume that the Chandrasekhar mass limit remains constant. This hypothesis is equivalent to assuming a constant G. This means that the "known" SN1a distances are model-dependent and cannot be used to test any epoch-dependent G model. They have to be corrected by introducing a model for the Absolute Luminosity G-dependence. HU provides this model in Appendix C.
3. Lunar Laser Ranging (LLR) data, which tracks changes in the Moon's orbit to estimate variations in Earth's moment of inertia and infer constraints on G.

This paper reevaluates these constraints and identifies key methodological flaws. We propose an alternative framework, the Hypergeometrical Universe (HU) model, which naturally incorporates an epoch-dependent G. The HU model replaces traditional assumptions with a dynamic framework where gravitational interactions evolve over time, providing a more consistent explanation for various cosmic phenomena.

2. Challenges to Conventional Constraints on G-Variability

2.1 The Young Faint Sun Paradox Reexamined

The Young Faint Sun Paradox arises from the standard stellar evolution model, which predicts that the Sun's luminosity was only 70% of its current value 4.5 billion years ago. This should have resulted in a frozen Earth, yet geological records show liquid water and early life. Conventional resolutions invoke high atmospheric CO_2 levels or methane-induced greenhouse warming, but these require fine-tuned conditions.

The HU model offers an alternative explanation: gradual hydrogen accretion by the Sun over billions of years. If the Sun started with a smaller mass and accreted hydrogen from the interstellar medium, its luminosity would have remained relatively stable, preventing extreme temperature variations on Earth. Additionally, if G was stronger in the past, stellar equilibrium conditions would have been different, naturally affecting solar luminosity.

2.2 Type Ia Supernovae and the Assumption of Constant G

SN1a explosions are used as standard candles in cosmology under the assumption that the Chandrasekhar mass limit is fixed. However, this limit depends on G:

$$M_{Ch} \propto G^{-3/2} \qquad (1)$$

Since SN1a luminosity is governed by the mass of the white dwarf at detonation, an epoch-dependent G would alter its absolute brightness. Using David Arnett's modeling, we derive the explicit G-dependence of SN1a luminosity and demonstrate that failing to account for this variation results in systematic biases

in photometric distance measurements. This suggests that cosmic acceleration inferred from SN1a dimming might be an artifact of improper calibration rather than evidence of dark energy.

2.3 Lunar Laser Ranging: A Flawed Constraint on G-Variability

LLR data is often cited as placing the strongest constraints on G-variability by measuring the recession rate of the Moon. However, the standard approach assumes conservation of total angular momentum while keeping G constant. In an epoch-dependent G framework, both the Earth's moment of inertia and the Moon's orbit evolve differently.

A proper treatment incorporating epoch-dependent G reveals that:

1. The expected variations in G are within the uncertainty of Earth's moment of inertia measurements.
2. NASA's LLR-based conclusions fail to model full angular momentum conservation under a varying G.
3. Observed lunar recession rates do not necessarily rule out a stronger G in the past.

Our results indicate that LLR does not provide a definitive constraint on G-variability and that improved precision is needed to test this hypothesis accurately.

3. The Hypergeometrical Universe Model and Its Implications

The HU model proposes a lightspeed-expanding hyperspherical universe where all matter consists of polymers of Fundamental Dilators. This model naturally incorporates an epoch-dependent G, altering fundamental interactions over cosmic time. HU replaces the traditional Big Bang paradigm with the Big Pop Cosmogenesis, which resolves inconsistencies in standard cosmology without requiring inflation, dark matter, or dark energy.

Among the many observations supporting HU is how HU's epoch-dependent G explains away the Great Attractor—a field of drift velocities reaching several hundred km/s without associated acceleration. This observation aligns with a stronger G in early cosmic history, providing further evidence for HU's epoch-dependent framework.

4. Conclusion

By critically reexamining traditional constraints on G-variability, we demonstrate that previous assumptions are flawed and overstated. The Young Faint Sun Paradox is naturally resolved by hydrogen accretion, SN1a standard candle assumptions fail to account for epoch-dependent G, and LLR constraints do not properly model angular momentum conservation. The HU model provides a consistent framework for addressing these issues and suggests that an evolving G is a necessary component of fundamental physics.

In addition to explaining the Great Attractor, SN1a distances without Space Stretching, Dark Matter or Dark Energy, Earth's Thermal History, Universe Creation and Evolution, Quantum Mechanics, and Quantum Gravitation, HU provides a Pati-Salam GUT SU(4) model for Particle Physics and a new Particle Taxonomy.

The laws of nature also support HU. These laws are a unique aspect of HU. No other theory derives the Laws of Nature from first principles. HU reproduced all successes of Quantum Electrodynamics, General Relativity, Special Relativity, and Big Bang Nucleosynthesis, and promises to revolutionize Plasma Physics and Nuclear Fusion.

Future research will extend this analysis to additional astrophysical phenomena and refine observational techniques to test epoch-dependent gravitational physics.

Appendix A: THE BIG POP COSMOGENESIS - PHENOMENOLOGY

1. Introduction

The Hypergeometrical Universe Theory (HU) proposes a novel cosmogenesis model, termed **The Big Pop**, as a paradigm shift from traditional cosmological models like the Big Bang. In contrast to singularities and inflationary models, HU offers a cohesive and simplified approach to the universe's creation and evolution. Here, we outline the principles, logic, and sequence of events that led to the formation and development of the universe under HU.

2. Hypotheses

HU's Big Pop Cosmogenesis is based on three core hypotheses:

- The universe exists as a lightspeed expanding hyperspherical hypersurface (LEHU).
- Matter is composed of **polymers of the Fundamental Dilator (FD)**, which are coherences between stationary states of deformation of space.
- FDs obey the **Quantum Lagrangian Principle (QLP)**, which dictates that no particle should perform or receive work from the constraints of space itself. This principle replaces all other physical laws within HU.

These hypotheses imply that HU creates Matter directly and simply from deformed space, resulting in a simplified universe where only Space, Deformed Space, and Time exist. **This is the simplest possible model for the Universe, and one can use Occam's Razor to assign it as the Theory of Everything.**

3. Stages of the Big Pop Cosmogenesis

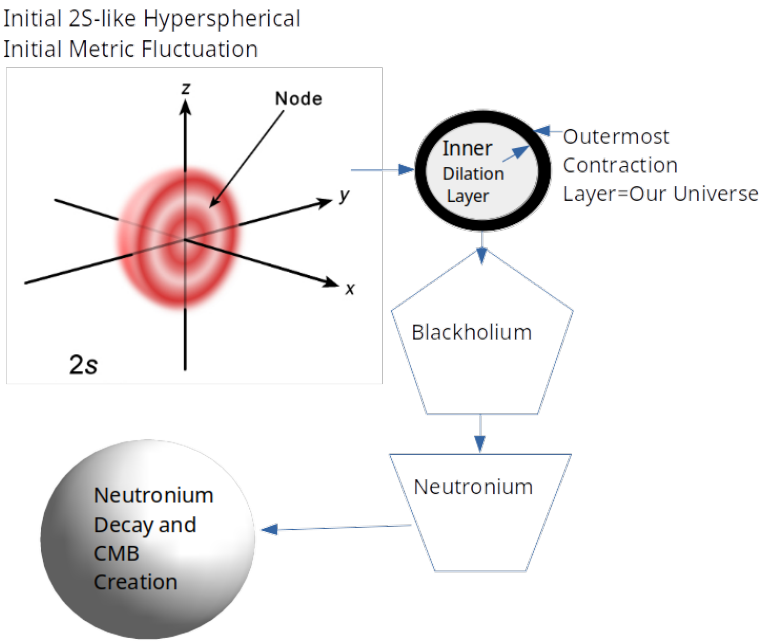

Figure 1. The Big Pop Cosmogenesis.

This shows the sequence of events associated with the lifetime of the Universe. HU proposes that the Universe started with a simple Heisenberg Principle Driven Hyperspherical Metric Fluctuation of 662 light-seconds 4D radius.

The Big Pop model describes the universe's formation through a series of stages:

- **Initial Metric Fluctuation**: HU proposes that the universe began as a 4D hyperspherical metric fluctuation around 14 billion years ago. This fluctuation featured dilation at the core and contraction at the outer layers. Without the infinite potential well typically associated with a singularity, the universe started with a temperature of zero Kelvin (because the Initial Metric Fluctuation contained no internal degrees of freedom), containing all the matter it would ever have.
- **Big Pop**: The Heisenberg principle dictates the Initial Metric Fluctuation followed by partial recombination. The partial recombination led to two remaining layers: the **Inner Dilation Layer (IDL)** and the **Outermost Contraction Layer (OCL)**. After the Big Pop, IDL pushed OCL and fragmented it, creating the Blackholium (hyperspherical Black Hole). No energy is required to create the universe. Matter, the positive contained in the OCL, is countered by the negative energy contained in the IDL.
- The Big Pop (partial recombination of dilation and contraction layers) is analogous to a **Prince Rupert's Drop**, the outermost contraction layer set into motion at lightspeed, forming a hyperspherical black hole known as **Blackholium**. The expanding hyperspherical locus of the Blackholium contains all of the universe's Matter. Notice that all particles surf the IDL, which expands radially at the speed of light.
- **Blackholium-Neutronium Phase Transition**: As the universe continued expanding, a phase transition occurred, converting Blackholium into **Neutronium**. This phase triggered **Neutronium Acoustic Oscillations (NAO)**, a key process that influenced the features observed in the Cosmic Microwave Background (CMB).
- **Neutronium Acoustic Freezing**: As the universe expanded further, the speed of sound in Neutronium matter dropped significantly, freezing the NAOs. These oscillations are modeled as hyperspherical harmonics, influencing the CMB's low-frequency components.
- **HU Big Bang**: Neutronium eventually decayed, releasing energy at the end of the first day and forming a hot hydrogen plasma, marking the HU equivalent of the Big Bang. The Neutronium evaporation lasted three days. Continued expansion led to the cooling of the Universe. This process leads to the Transparency Epoch, when the universe cooled enough for light to propagate freely.

The neutronium acoustic oscillations are sensitive to the speed of sound in the neutron matter.

This fragmentation process inherently selects matter (protons as contractions and electrons as dilations) over antimatter due to the symmetrical but phase-aligned nature of the Fundamental Dilator Coherence. This mechanism negates the possibility of antimatter creation under the initial conditions, thereby naturally explaining the observable matter dominance in the universe.

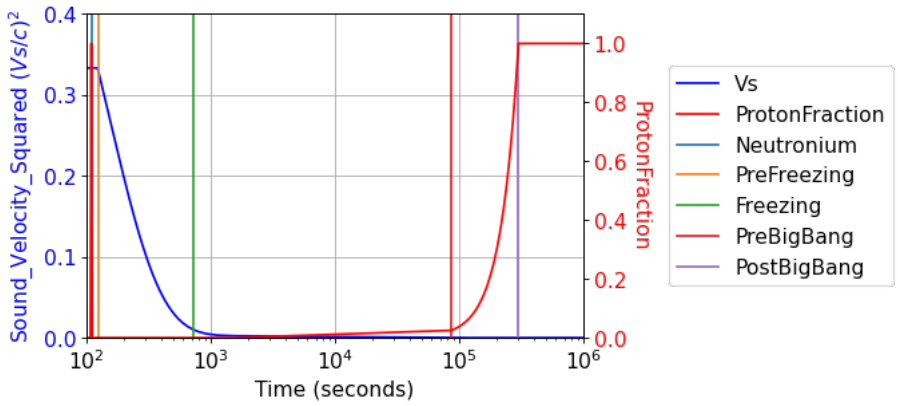

Figure 2. Plotting showing the square of the speed of sound inside a Neutronium Phase.

This figure shows the relationship between the speed of sound squared inside the Neutronium phase as a function of the time. It takes into consideration the lightspeed expansion.

Around 300 MeV/fm^3 (around 100 seconds after the Big Pop), the speed of sound changes abruptly, freezing in place neutronium acoustic oscillations. NAOs are construed to be the reason for the observed features of the cosmic microwave background. They are modeled as hyperspherical harmonics. This figure also shows the Neutronium Decay and the rise of the Proton Fraction, which is the reason for the heating up of the Universe in the HU Big Bang.

4. Cosmological Implications

The Big Pop model offers several insights and implications:

- **Baryonic Acoustic Oscillations (BAO)**: The decay of Neutronium initiated Baryonic Acoustic Oscillations, distinct from the Neutronium Acoustic Oscillations. HU models these as hyperspherical harmonics, matching the observed features in the CMB as recorded by satellites like Planck.
- **Epoch-Dependent G and SN1a Reinterpretation**: HU's model includes an epoch-dependent gravitational constant G. This implies that Type Ia Supernovae (SN1a), traditionally used as standard candles, should have their photometric distances recalculated based on the epoch's value of G ($G^{-3/2}$). This adjustment eliminates the need for dark matter and dark energy to explain the data (see Appendix B for details). It also corrects the Cosmic Distance Ladder, removing inconsistencies related to distances exceeding the speed of light.
- **Simplification of Cosmogenesis**: The Big Pop eliminates the need for speculative constructs like inflation, false vacuum decay, and singularities. By positing that the universe formed from a neutral initial metric fluctuation, HU provides a coherent and less parameterized model that adheres to Occam's Razor.

5. The Birth of Blackholium: The Prince Rupert's Drop Analogy

As the outermost contraction layer expanded, propelled by the inner dilation layer, it formed **Blackholium**, a hyperspherical black hole. This process can be analogized with **Prince Rupert's Drop**, where the smooth outer layer undergoes rapid expansion. At this moment, the universe was born with zero entropy—no internal degrees of freedom existed initially.

Further expansion led to the phase transition from Blackholium to Neutronium, where the emission of electron neutrinos enabled neutrons to form. These transitions played a critical role in the subsequent evolution of the universe's structure.

6. Modeling and Observations

The Neutronium phase and its transitions are modeled using hyperspherical harmonics and acoustic oscillations. By filtering the CMB's low-frequency components (up to k=48), HU identifies and simulates the features observed by the Planck Satellite. The alignment of these simulations with observed data supports HU's Big Pop model as a viable alternative to the inflationary Big Bang paradigm.

7. The modeling of the Neutronium Acoustic Oscillations

Since the Blackholium-Neutronium-phase-transition-induced sound waves take place in 4D, the natural basis to represent them is Hyperspherical Harmonics[38]. Hyperspherical Harmonics are defined by three quantum numbers (k, l, m).

The modeling of the CMB required filtering the CMB low-frequency components (up to k=9) and a grid search to find the proximity of our locus (Earth location). This corresponds to the initial random walk to find the "You Are Here" sign.

After the localization of our neighborhood, I increased the maximum value of k to 48 and performed further refining of our position. That was the limit that I could achieve using my available computing power.

7.1 Earth's Location (You Are Here)

The 4D radius is 14.03 billion light-years. The best site for Earth is shown below:

$$\chi = 339.46 \text{ degrees}$$

$$\theta = 341.1 \text{ degrees}$$

$$\phi = 104.08 \text{ degrees} \qquad (2)$$

Here are the Cosmic Microwave Background observations by the Planck Satellite and HU simulation using Hyperspherical Harmonics:

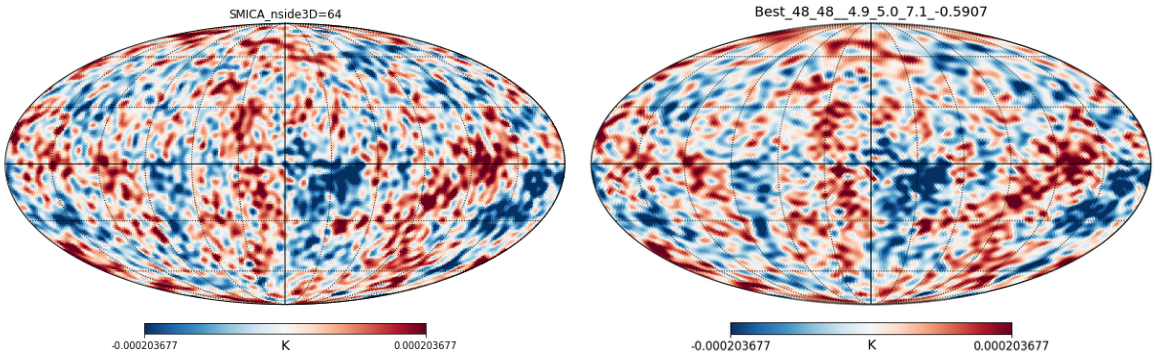

Figure 3. Planck Satellite CMB observation and hyperspherical harmonics simulation result.

This figure shows Planck Satellite CMB observation filtered to show the low-frequency components and the simulation using hyperspherical harmonics (up to k=48).

The Neutronium decay results in the Baryonic Acoustic Oscillations and corresponds to the difference between these two images:

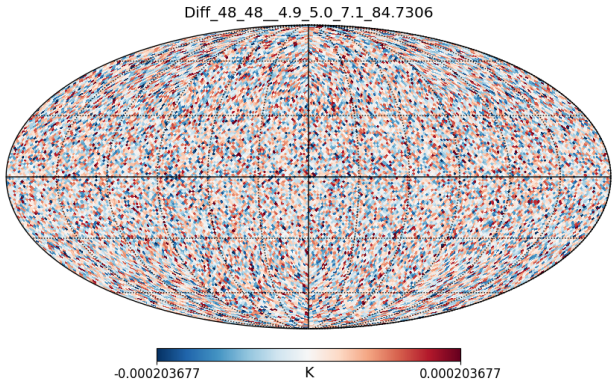

Figure 4. Difference between Planck Satellite Observation and Simulated CMB.

This figure shows the difference between observations and low-frequency simulation. The high-frequency waves were produced when the Neutronium evaporated and released the 0.78 MeV per neutron. It also created the Baryonic Acoustic Oscillations related to Neutronium decay. The modeling of BAO is not relevant to the Hypergeometrical Universe Theory. The only difference is how one attributes the low-frequency modulation. The current model assigns them to "Quantum Fluctuations," and HU attributes them to Neutronium Acoustic Oscillations – and quantifies those 4D sounds.

7.2 Big Bang Nucleosynthesis

The first time the universe is heated was during the Neutronium Evaporation Event. It happened at the end of the first day and lasted three days. Each neutron released 0.78MeV, which is the required and sufficient condition for Big Bang Nucleosynthesis.

Here, we present the comparison between the universe's conditions and the center of the Sun:

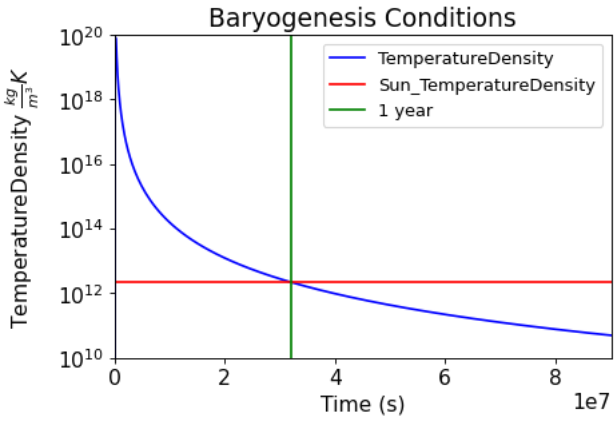

Figure 5. Plot of the product Density-Temperature in the universe.

This figure shows the evolution of the universe in terms of temperature and density. The red line corresponds to the value at the center of the Sun. The vertical green line marks the one-year mark. So, the Universe was much hotter and denser than the core of the sun for more than a year. In the early days, it was some 10 million times that value. The limited amount of time and temperature*density allows for the nucleosynthesis not to follow a Boltzmann distribution and explains why there is less Lithium than one would expect if nucleotides were in equilibrium.

8. Dimensionality Probability Distribution Function

HU proposes a probabilistic model for Dimensionality. Dimensionality is mapped to natural numbers, and they run all the way to infinity. If the probability distribution were uniform (the simplest possible model), then our 4D Universe would be infinitely unlikely. HU maps the volume of a unitary radius n-dimensional hypersphere to the accessible volume. In other words, momentum is not limited in the phase space. That said, space allocation to each state is. So, the probability of a given dimension is proportional to the volume of the unitary radius n-dimensional sphere. The probability distribution is shown in the figure below.

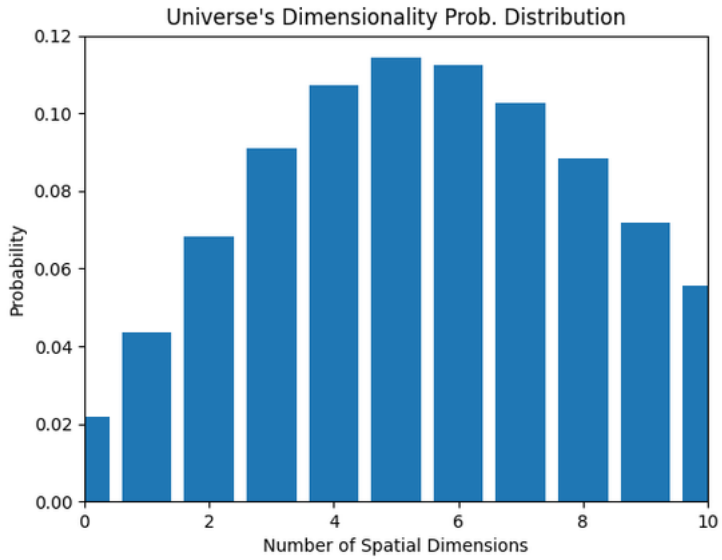

Figure 6. Dimensionality Probability Distribution proportional to the n-dimensional volume of a unitary n-hypersphere.

9. Conclusions

The Big Pop Cosmogenesis offers a simplified and consistent model for the creation and evolution of the universe. By eliminating the need for singularities, dark matter, dark energy, and inflation, HU adheres to the principles of simplicity and consistency. It aligns with observable phenomena, such as the CMB and supernova data, providing a cohesive framework that stands as a viable alternative to the current cosmological models.

Appendix B: Reevaluating Laser Lunar Ranging Analysis

TLM assumes that the Moon obeyed Kepler's Law:

$$r^3 n^2 = GM \tag{3}$$

From this equation and the consideration that G might vary, one can easily derive:

$$3\frac{\dot{r}}{r} + 2\frac{\dot{n}}{n} = \frac{\dot{G}}{G} \tag{4}$$

NASA observed:

$$\frac{\dot{r}}{r} = 1.0\text{E-}10 \tag{5}$$

$$\frac{\dot{n}}{n} = -1.5E-10 \tag{6}$$

They concluded that:

$$\frac{\dot{G}}{G} \approx 0 \tag{7}$$

What is wrong with that reasoning?

The observed values were implicitly considered not to have any G-dependence. The correct reasoning would have been:

$$\frac{\dot{r}}{r} = \left(\frac{\dot{r}}{r}\right)_{tlm} + \left(\frac{\dot{r}}{r}\right)_{G} = 1.0E-10 \tag{8}$$

$$\frac{\dot{n}}{n} = \left(\frac{\dot{n}}{n}\right)_{tlm} + \left(\frac{\dot{n}}{n}\right)_{G} = 1.5E-10 \tag{9}$$

All observations should always be considered to be G-dependent when evaluating a G-dependent model or the variability of Newton's Gravitational Constant G.

So, equation (4) becomes:

$$3\left(\frac{\dot{r}}{r}\right)_{tlm} + 2\left(\frac{\dot{n}}{n}\right)_{tlm} = 0 \tag{10}$$

Equation (4) satisfies LLR expectations, while equation (11) should be satisfied by the modeling of Keplerian Orbits under epoch-dependent G.

$$3\left(\frac{\dot{r}}{r}\right)_{G} + 2\left(\frac{\dot{n}}{n}\right)_{G} = \frac{\dot{G}}{G} \tag{11}$$

This equation would be satisfied if:

$$\left(\frac{\dot{r}}{r}\right)_G = \frac{\dot{G}}{G} \tag{12}$$

and

$$\left(\frac{\dot{n}}{n}\right)_G = -\frac{\dot{G}}{G} \tag{13}$$

That is exactly what one would expect from using angular momentum conservation for the Moon's orbit as an approximation:

$$\left(\frac{\dot{n}}{n}\right)_G = -\left(\frac{\dot{r}}{r}\right)_G \tag{14}$$

In other words, a simple angular moment approximation would indicate that TLM could add epoch-dependent G modeling and not have any mismatch between the model prediction and the observed elliptical orbit. The actual values for the G-dependent contributions cannot be ascertained just by the Moon's angular momentum conservation. Hence, these are just initial estimates or proof of principle.

Due to Tidal Locking, individual angular momenta are not conserved. Hence, one needs to consider the conservation of total angular momentum:

$$\frac{d}{dt}\left(L_{orb} + L_{\Theta} + L_{Moon}\right) = 0 \tag{15}$$

Since the Moon spinning angular momentum is much smaller than the other contributions, we will neglect it, as it was done in TLM:

$$\frac{d}{dt}\left(L_{Moon}\right) << \frac{d}{dt}\left(L_{orb} + L_{\Theta}\right) \tag{16}$$

Notice that whenever a total value for an observable is available, that will be used

So:

$$\frac{1}{L_{orb}}\frac{d}{dt}\left(L_{\Theta}\right) \cong -\frac{1}{L_{orb}}\frac{d}{dt}\left(L_{orb}\right) \tag{17}$$

With

$$L_{orb} = Mr^2 n \tag{18}$$

So:

$$\frac{1}{L_{orb}}\frac{d}{dt}\left(L_{orb}\right) = -\left(2\frac{\dot{r}}{r} + \frac{\dot{n}}{n}\right) = \text{-5E-11} \tag{19}$$

So, equation (17) becomes:

$$\frac{d}{dt}\left(L_{\Theta}\right) \cong \text{-5.0E-11} \cdot L_{orb} \tag{20}$$

$$\frac{d}{dt}\left(I_{\Theta}\Omega_{\Theta}\right) \cong \text{-5E-11} \cdot L_{orb} \tag{21}$$

$$I_{\Theta}\dot{\Omega}_{\Theta} + \dot{I}_{\Theta}\Omega_{\Theta} = -\ 5.0\text{E-11} \cdot L_{orb} \tag{22}$$

$$\left[\left(\frac{\dot{\Omega}_{\Theta}}{\Omega_{\Theta}} + \frac{\dot{I}_{\Theta}}{I_{\Theta}}\right)_{tlm} + \left(\frac{\dot{\Omega}_{\Theta}}{\Omega_{\Theta}} + \frac{\dot{I}_{\Theta}}{I_{\Theta}}\right)_{G}\right] = -\ 5.0\text{E-11} \cdot \frac{L_{orb}}{L_{\Theta}} \tag{23}$$

$$\left[\left(\frac{\dot{I}_{\Theta}}{I_{\Theta}}\right)_{tlm} + \left(\frac{\dot{I}_{\Theta}}{I_{\Theta}}\right)_{G}\right] = -\ 5.0\text{E-11} \cdot \frac{L_{orb}}{L_{\Theta}} - \left[\left(\frac{\dot{\Omega}_{\Theta}}{\Omega_{\Theta}}\right)_{tlm} + \left(\frac{\dot{\Omega}_{\Theta}}{\Omega_{\Theta}}\right)_{G}\right] \tag{24}$$

Earth fractional angular acceleration is measured using atomic clocks:

$$\Omega_{\theta} = \frac{2\pi}{T} \Rightarrow \frac{\dot{\Omega}_{\theta}}{\Omega_{\theta}} = -\ \frac{\dot{T}}{T} \tag{25}$$

Resulting:

$$\left[\left(\frac{\dot{\Omega}_{\Theta}}{\Omega_{\Theta}}\right)_{tlm} + \left(\frac{\dot{\Omega}_{\Theta}}{\Omega_{\Theta}}\right)_{HU}\right] = -\ \frac{\dot{T}}{T} = -\ \frac{\left(\dfrac{\text{1.7E-3}}{(\,100 \cdot 365.2425 \cdot Day)}\right)}{Day} = \text{-4.65E-8} \tag{26}$$

Since:

$$I_{\Theta} = CM_{\Theta}R_{\Theta}^{\,2} \tag{27}$$

One still needs to create a model for the variation of Earth's moment of inertia with varying G:

$$\left(\frac{\dot{I}_{\Theta}}{I_{\Theta}}\right)_{G} = \left(\frac{d\ln\left(I_{\Theta}\right)}{dt}\right)_{G} = 2\left(\frac{\dot{R}_{\Theta}}{R_{\Theta}}\right)_{G} = -\ \frac{\dot{G}}{G} \tag{28}$$

Here, we will consider that the inside of Earth is under a hydrostatic equilibrium that is not unlike the one in White Dwarfs and use the Chandrasekhar Radius G-dependence:

$$\left(\frac{\dot{R}_{\Theta}}{R_{\Theta}}\right)_{G} = -\ \frac{1}{2}\frac{\dot{G}}{G} \tag{29}$$

$$\left(\frac{\dot{I}_{\Theta}}{I_{\Theta}}\right)_{tlm} = -\ 5.0E-11 \cdot \frac{L_{orb}}{L_{\Theta}} - \left[\left(\frac{\dot{\Omega}_{\Theta}}{\Omega_{\Theta}}\right)_{tlm} + \left(\frac{\dot{\Omega}_{\Theta}}{\Omega_{\Theta}}\right)_{G}\right] + \frac{\dot{G}}{G} \tag{30}$$

The effect of Relativity in the calculations of the moment of inertia variation is

$$\frac{L_{orb}}{L_{\Theta}} = 0.2034 \tag{31}$$

$$\left(\frac{\dot{\Omega}_{\Theta}}{\Omega_{\Theta}}\right) = \left[\left(\frac{\dot{\Omega}_{\Theta}}{\Omega_{\Theta}}\right)_{tlm} + \left(\frac{\dot{\Omega}_{\Theta}}{\Omega_{\Theta}}\right)_{HU}\right] = -4.65E-8 \tag{32}$$

$$\frac{\dot{G}}{G} = -\frac{1}{14.04E9} = \text{-7.12E-11} \tag{33}$$

$$\frac{\left(\frac{\dot{I}_{\theta}}{I_{\theta}}\right)_{\text{tlm},G}}{\left(\frac{\dot{I}_{\theta}}{I_{\theta}}\right)_{\text{tlm}}} = \frac{\frac{\dot{G}}{G}}{\text{-5.0E-11}\,\frac{L_{\theta}}{L_{\text{orb}}} - \left[\left(\frac{\dot{\Omega}_{\theta}}{\Omega_{\theta}}\right)_{\text{tlm}} + \left(\frac{\dot{\Omega}_{\theta}}{\Omega_{\theta}}\right)_{G}\right]} = 0.15\% \tag{34}$$

This means that a fully epoch-dependent G Tidal Locking Model would be consistent with observations and differ from the constant-G TLM by less than 0.2% in their prediction of the variation of Earth's Moment of Inertia.

This implies that the NASA Tidal Locking Laser Lunar Ranging Experiment couldn't possibly detect the effect of Gravitational Changes. The experiment wasn't precise enough because the rate of change of Earth's Moment of Inertia is not known with less than 0.2% precision.

In other words, all observables are recovered and are very resilient to changes in G. Notice that in the derivation using the conservation of global angular momentum, the results from equations (3) and (4) were not used since Kepler's Law is not a good enough description of the Moon's orbit, within this context.

Appendix C: Faint Young Sun Paradox Objection

1. The Conventional Young Faint Sun Paradox

The Young Faint Sun Paradox arises from the observation that standard stellar evolution models predict that the Sun's luminosity was only 70% of its current value about 4.5 billion years ago. This presents a major problem: Earth should have been frozen for much of its early history with a significantly dimmer Sun, contradicting geological and biological evidence of liquid water and early life.

Standard models introduce additional greenhouse warming mechanisms, such as higher atmospheric CO2 or methane concentrations, to resolve this paradox. However, these explanations remain speculative and require fine-tuned conditions to maintain a stable temperature over billions of years.

2. A New Resolution: Continuous Hydrogen Accretion onto the Sun

The Hypergeometrical Universe (HU) model provides a natural resolution to the paradox by introducing a hydrogen accretion mechanism. Instead of assuming the Sun was born with its full mass, HU proposes that it gradually accreted hydrogen from the interstellar medium over 4.5 billion years.

This accretion process allows for:

- A continuously increasing **solar mass** over time.
- A compensating effect for a potentially stronger **gravitational constant G in the past**, which would have otherwise led to increased luminosity.
- A natural explanation for the **observed constancy of Earth's temperature** over billions of years without requiring fine-tuned greenhouse effects.

3. Estimating the Hydrogen Accretion Rate

- If the Sun **started at 0.7 Solar Mass** and gradually increased to its current mass (1.0 **Solar Mass**), its luminosity would have remained **roughly constant over time**, preventing extreme temperature variations on Earth.
- The required average hydrogen accretion rate is 1.08 micrograms per second per square meter of solar surface.
- This rate aligns with plausible astrophysical processes, including the **infall of interstellar hydrogen** as the Sun orbits the Milky Way.
- The smaller cross-section of neutral hydrogen rejects objections associated with the drag by the outgoing Solar Wind.

4. The Role of Epoch-Dependent G in Solar Evolution

In the HU model, Newton's gravitational constant decreases over time as the universe expands, following:

$$G(z) = G_0(1+z) \tag{35}$$

This means that in the early solar system, G was stronger than today, influencing the equilibrium radius and luminosity of the Sun. With a stronger G:

- The early Sun would have been more compact for the same mass.
- The Chandrasekhar mass limit would have been lower, affecting nuclear fusion rates.
- The balance between accretion and gravitational binding energy ensures a stable energy output.

5. Implications for Other Star Systems and Exoplanet Habitability

If the hydrogen accretion mechanism proposed in HU applies universally, it may have profound implications for:

- **Other stars:** Lower-mass stars could accrete mass over time, altering our understanding of stellar lifetimes and evolution.
- **Exoplanet habitability:** Planets around young stars may experience more stable climates if their host stars gradually accrete mass.
- **The Fermi Paradox:** The evolution of planetary systems under an evolving G and accreting stars could affect the emergence and longevity of life. In addition, in the early universe, the natural relative weakening of Gravity was faster, shifting the Goldilocks region too fast for life to evolve.

6. Conclusion

The Young Faint Sun Paradox is not a paradox at all when one considers a model where:

- The Sun was born smaller and gradually accreted hydrogen, increasing its mass over time.
- G was stronger in the past, modifying the solar equilibrium conditions.

The combined effects stabilized Earth's climate, eliminating the need for speculative greenhouse gas explanations.

This solution aligns with both astrophysical constraints and geological evidence of stable temperatures on Earth, offering a paradigm shift in our understanding of stellar evolution.

Hydrogen Rain also explains the extra acceleration given to the Oumuamua asteroid on its way out.

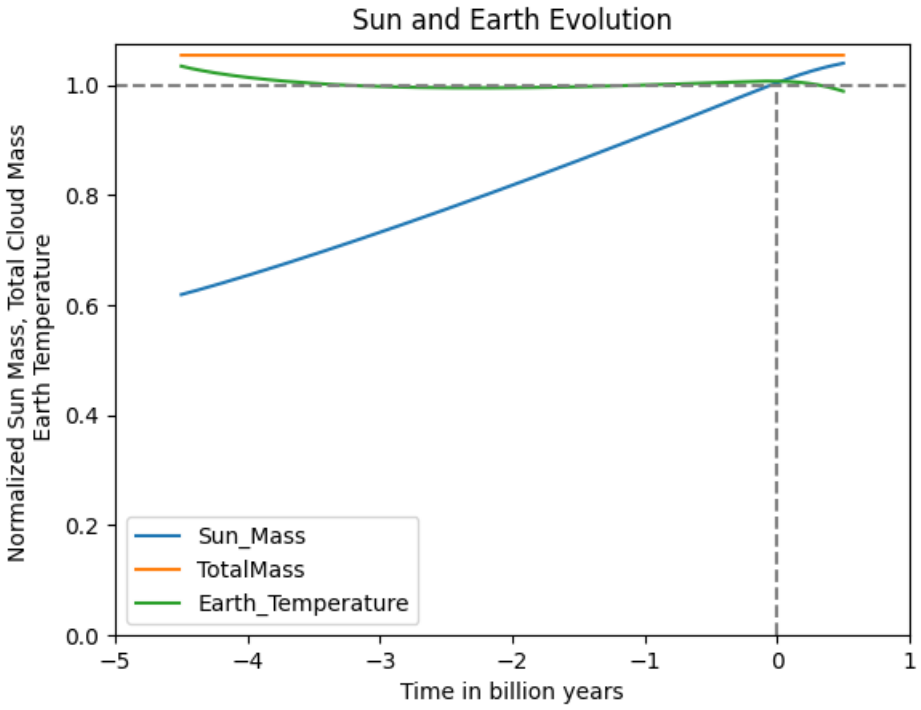

Figure 7. Here we see Earth's average temperature as a function of time while the Sun accreted 0.4 Solar Masses in 4 billion years.

This figure shows that the Early Sun wasn't unexpectedly weak (Faint Young Sun Paradox). The increasing Sun mass compensates for the decreasing G. A continuous rate of hydrogen rain is what one would expect if the rain is coming from a larger environmental reservoir distributed along the sun's path around the galaxy. The sun travels around the galaxy every 250 million years and thus makes 16 roundtrips around the Milky Way.

Appendix D: The SN1a Objection

1. The Stellar Candles Hypothesis and Its Implicit Assumption of Constant G

The authors assume that SN1a explosions consistently produce the same absolute luminosity regardless of redshift. This assumption is expressed explicitly in their caveat:

"An important caveat is that it rests on the assumption that the same mass of ^{57}Ni is burned to create the standard candle regardless of redshift."

This statement effectively embeds the **Stellar Candles Hypothesis**, which assumes that the Chandrasekhar Mass Limit—and thus the supernova's peak luminosity—remains unchanged. However, the Chandrasekhar limit is explicitly **G-dependent** and scales as follows:

$$M_{\mathrm{Ch}} \propto G^{-3/2} \tag{36}$$

Since the energy release and absolute luminosity of an SN1a explosion depend on M_{Ch}, the peak brightness should also exhibit a clear dependence on G, contradicting the assumption of a fixed standard candle. So, the article's postulated hypothesis precluded a real test of the variability of G.

2. Deriving the Correct G-Dependence for SN1a Absolute Luminosity

Using the framework established by Arnett (1980), we derive the explicit relationship between SN1a luminosity and G. The key result is that the **absolute luminosity of SN1a varies with epoch-dependent G** as:

$$L_{\mathrm{SN1a}} \propto G^{n}, \quad \text{with} \quad 3 \leq n \leq 3.5 \tag{37}$$

This correction significantly alters photometric distance estimates. Since current supernova cosmology assumes a constant G, distances to SN1a-hosting galaxies have been systematically overestimated.

3. Consequences for Cosmology and the Dark Energy Interpretation

The failure to account for G-dependence in SN1a luminosity artificially inflates distances, leading to the apparent acceleration of the universe's expansion. This provides an **alternative explanation for the need to introduce dark energy** in the ΛCDM model. If the observed dimming of SN1a is partially due to an evolving G, then the inferred acceleration of the universe may be an artifact of an incomplete distance calibration rather than evidence of dark energy.

Appendix E: Derivation of the Absolute Luminosity SN1a G-Dependence.

We will base our derivation on Arnett's work: Here, we will study the effect of a distinct value of G on the Light Curve. The Luminosity of a Supernova is given by Arnett's eq.39:

$$L(1,t) = L(1,0)\phi(t) \tag{38}$$

where

$$L(1,0) = K_0\left[\frac{R(0)}{10^{14}\,cm}\right]\left[\frac{E_{th}(0)}{10^{51}\,ergs}\right]\left(\left[\frac{0.4cm^2\,g^{-1}}{\kappa}\right]\right)\left[\frac{1M_{\Theta}}{M}\right] \tag{39}$$

$$E_{th}(0) = \int_0^{R(0)} aT^4 4\pi r^2 dr \tag{40}$$

Chandrasekhar Radius has the following G dependence:

$$R^{Epoch}_{Chandrasekhar} = \left(\frac{G_0}{G_{Epoch}}\right)^{\frac{1}{2}} R_{Chandrasekhar} = \vartheta R_{Chandrasekhar} \tag{41}$$

$$\vartheta = \left(\frac{G_0}{G_{Epoch}}\right)^{\frac{1}{2}} = \frac{R^{Epoch}_{Chandrasekhar}}{R_{Chandrasekhar}} \tag{42}$$

If you model a Star as to be emitting Blackbody radiation, its luminosity will be given by:

$$L = 4\pi R^2 \sigma T_s^{\,4} \tag{43}$$

Relating two stars in different epochs facing different G_s, same temperature T_{Solar}, we obtain:

$$\frac{L^{Epoch}_{Solar}}{L_{Solar}} = \left(\frac{R^{Epoch}_{Chandrasekhar}}{R_{Chandrasekhar}}\right)^2\left(\frac{T^{Epoch}_{Solar}}{T_{Solar}}\right)^4 = \left(\frac{R^{Epoch}_{Chandrasekhar}}{R_{Chandrasekhar}}\right)^2 = \vartheta^2 \tag{44}$$

1. LOW RADIATION PRESSURE LIMIT

Simple modeling of the Sun's luminosity yields[13]:

$$L \propto G^4 M^{-3.33} \tag{45}$$

Considering the ratio between luminosities to scale with Mass we can derive the epoch dependent Solar Mass:

$$\left(\frac{G_{Epoch}}{G_0}\right)^4\left(\frac{M_\Theta^{Epoch}}{M_\Theta}\right)^{3.33}=\frac{L_{Solar}^{Epoch}}{L_{Solar}}=\left(\frac{R_{Chandrasekhar}^{Epoch}}{R_{Chandrasekhar}}\right)^2\left(\frac{T_{Solar}^{Epoch}}{T_{Solar}}\right)^4=\left(\frac{R_{Chandrasekhar}^{Epoch}}{R_{Chandrasekhar}}\right)^2=\vartheta^2 \quad (46)$$

This Solar mass is the mass required to yield the same surface temperature, given that the radius shrank according to the White Dwarf Chandrasekhar radius. The approximation is that Luminosity scales with Star mass.

$$M_\Theta=\vartheta^{-3}M_\Theta^{Epoch} \quad (47)$$

Substituting equations (41)(42), (47) into equation (39):

$$L(1,0)=K_0\left[\frac{\vartheta^{-1}R_{Chandrasekhar}^{Epoch}(0)}{10^{14}\,cm}\right]\left[\frac{\vartheta^{-3}E_{th}^{Epoch}(0)}{10^{51}\,ergs}\right]\left(\left[\frac{0.4cm^2g^{-1}}{\kappa}\right]\right)\left[\frac{1\vartheta^{-3}M_\Theta^{Epoch}}{M}\right] \quad (48)$$

$$L(1,0)=\vartheta^{-7}K_0\left[\frac{R_{Chandrasekhar}^{Epoch}(0)}{10^{14}\,cm}\right]\left[\frac{E_{th}^{Epoch}(0)}{10^{51}\,ergs}\right]\left(\left[\frac{0.4cm^2g^{-1}}{\kappa}\right]\right)\left[\frac{1M_\Theta^{Epoch}}{M}\right] \quad (49)$$

Since

$$L^{Epoch}(1,0)=K_0\left[\frac{R_{Chandrasekhar}^{Epoch}(0)}{10^{14}\,cm}\right]\left[\frac{E_{th}^{Epoch}(0)}{10^{51}\,ergs}\right]\left(\left[\frac{0.4cm^2g^{-1}}{\kappa}\right]\right)\left[\frac{1M_\Theta^{Epoch}}{M}\right] \quad (50)$$

We obtain the following relationship between Absolute Peak Luminosities now and in earlier epochs:

$$L^{Epoch}(1,0)=\vartheta^7L(1,0)=\left(\frac{G_0}{G_{Epoch}}\right)^{3.5}L(1,0)=\left(\frac{R^{Epoch}(0)}{R(0)}\right)^{3.5}L(1,0) \quad (51)$$

Where $R^{Epoch}(0)$ and R(0) are the 4D radius of the Universe at the epoch and now.

2. HIGH RADIATION PRESSURE LIMIT

For larger stars or during Supernova detonation, the radiation pressure is larger than the gas pressure in the radiation zone. Plugging in the radiation pressure instead of the ideal gas pressure used above yields:

$$L \propto M \quad (52)$$

Considering the ratio between luminosities to scale with Mass, we can derive the epoch dependent Solar Mass:

$$\left(\frac{M_{\Theta}^{Epoch}}{M_{\Theta}}\right)=\frac{L_{Solar}^{Epoch}}{L_{Solar}}=\left(\frac{R_{Chandrasekhar}^{Epoch}}{R_{Chandrasekhar}}\right)^{2}\left(\frac{T_{Solar}^{Epoch}}{T_{Solar}}\right)^{4}=\left(\frac{R_{Chandrasekhar}^{Epoch}}{R_{Chandrasekhar}}\right)^{2}=\vartheta^{2} \quad (53)$$

This Solar mass is the mass required to yield the same surface temperature, given that the radius shrank according to the White Dwarf Chandrasekhar radius. The approximation is that Luminosity scales with Star mass.

$$M_{\Theta}=\vartheta^{-2}M_{\Theta}^{Epoch} \quad (54)$$

Substituting equations (41)(42), (54) into equation (39):

$$L(1,0)=K_{0}\left[\frac{\vartheta^{-1}R_{Chandrasekhar}^{Epoch}(0)}{10^{14}\,cm}\right]\left[\frac{\vartheta^{-3}E_{th}^{Epoch}(0)}{10^{51}\,ergs}\right]\left(\left[\frac{0.4cm^{2}g^{-1}}{\kappa}\right]\right)\left[\frac{1\vartheta^{-2}M_{\Theta}^{Epoch}}{M}\right] \quad (55)$$

$$L(1,0)=\vartheta^{-6}K_{0}\left[\frac{R_{Chandrasekhar}^{Epoch}(0)}{10^{14}\,cm}\right]\left[\frac{E_{th}^{Epoch}(0)}{10^{51}\,ergs}\right]\left(\left[\frac{0.4cm^{2}g^{-1}}{\kappa}\right]\right)\left[\frac{1M_{\Theta}^{Epoch}}{M}\right] \quad (56)$$

Since

$$L^{Epoch}(1,0)=K_{0}\left[\frac{R_{Chandrasekhar}^{Epoch}(0)}{10^{14}\,cm}\right]\left[\frac{E_{th}^{Epoch}(0)}{10^{51}\,ergs}\right]\left(\left[\frac{0.4cm^{2}g^{-1}}{\kappa}\right]\right)\left[\frac{1M_{\Theta}^{Epoch}}{M}\right] \quad (57)$$

We obtain the following relationship between Absolute Peak Luminosities now and in earlier epochs:

$$L^{Epoch}(1,0)=\vartheta^{6}L(1,0)=\left(\frac{G_{0}}{G_{Epoch}}\right)^{3}L(1,0)=\left(\frac{R^{Epoch}(0)}{R(0)}\right)^{3}L(1,0) \quad (58)$$

This means that prior epochs had dimer Absolute Peak Luminosity and thus were overestimated by current Cosmology.

This means that Supernova Distances would be overestimated by $\left(\frac{R^{Epoch}(0)}{R(0)}\right)^{1.75}$ or $\left(\frac{R^{Epoch}(0)}{R(0)}\right)^{1.5}$ depending on the model one chooses for how the Mass of a Star would depend upon G.

The Supernova data indicates that the best value would be

$$d^{Epoch}(z)=\left(\frac{R^{Epoch}(0)}{R(0)}\right)^{1.66}d(z) \quad (59)$$

Which is between by $\left(\frac{R^{Epoch}(0)}{R(0)}\right)^{1.75}$ and $\left(\frac{R^{Epoch}(0)}{R(0)}\right)^{1.5}$.

Notice that in my derivation, I always considered that the redshift z was calculated in the Absolute Reference Frame. That is not the case in the Supernova Cosmology Project, but it is in the Pantheon Survey. The fitting of the Pantheon Survey data matches the lower range of HU's predictions.

$$d^{Epoch}(z) = \left(\frac{R^{Epoch}(0)}{R(0)}\right)^{1.5} d(z) = \left(\frac{1}{(1+z)}\right)^{1.5} d(z) \quad (60)$$

3. SN1a Analysis - The Strongest Test to HU's Epoch-Dependent G Model

The Hypergeometrical Universe Theory has been tested through observations that are much more sensitive to G-variability than the Laser Lunar Ranging Survey. HU correctly predicts the Type 1a Supernova distances starting from their redshifts using both the Pantheon Survey and the Supernova Cosmology Project data:

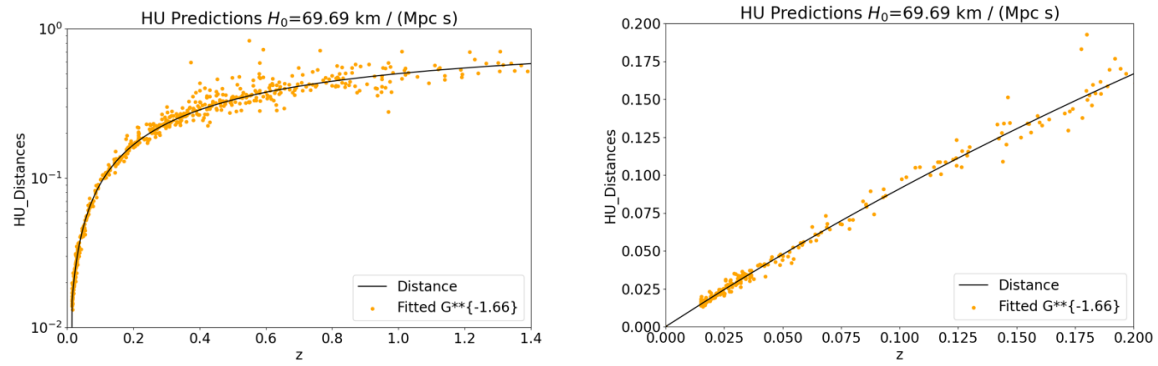

Figure 8. HU predictions for SN1a distances from the corresponding redshifts z (Supernova Cosmology Project dataset).

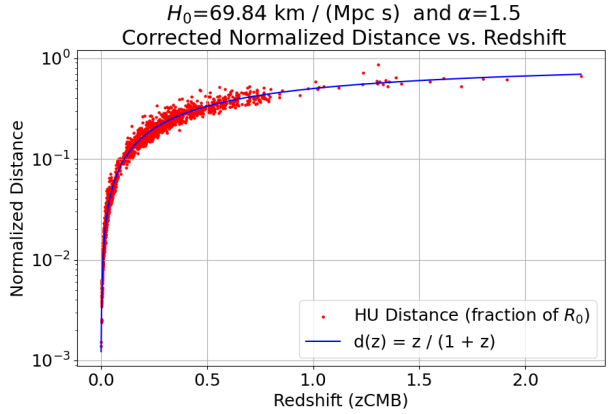

Figure 9. HU predictions for SN1a distances from the corresponding redshifts z (Pantheon Survey Dataset).

The original data (photometric Distances) were scaled using the epoch-dependent G. HU predicted the SN1a's Absolute Luminosity to have a G-dependence between G^{-3} and $G^{-3.5}$.

The 4D radius of the Universe is calculated simply as:

$$R(z) = R_0 \frac{z}{(1+z)} \quad (61)$$

Where R_0 is the 4D radius of the Universe. Since HU proposes the Universe to be a Lightspeed Expanding Hyperspherical Hypersurface (LEHU topology), then R_0 is related to Hubble's Constant H_0 through:

$$H_0 = \frac{c}{R_0} \qquad (62)$$

Where c is the speed of light.

HU derived the Laws of Nature, and Newton's Gravitational Constant became inversely proportional to the 4D radius:

$$G(z) = G_0 (1+z) \qquad (63)$$

Notice that the fitting scales the distances with G1.5; that is, the current photometric distances overestimate them by that factor.

4. HU Replaces Photons by 4D Quantum Metric Waves.

HU derivation also implies that photons are part of a larger quantum construct: a 4D Metric Wave instead of being a solitonic packet of energy. Since all particles are surfing the Inner Dilation Layer, there is nothing to dephase (extract energy) from the metric wave outside the 3D hypersurface. Conceptually, that is the reason why fields decay with inverse quadratic distance instead of inverse cubic distance. The field outside the hypersurface will never lose energy.

The 4D Metric Wave construct easily explains any non-local property of light (e.g., Quantum Entanglement) because the construct is inherently delocalized.

In other words, HU extended the range of light into the 4D space while fixing all particles onto a 4D-lightspeed-expanding-hyperspherical metric fluctuation. That is consistent with HU recasting of particles as coherences between stationary states of deformation of space. So, particles are metric wave generators called Fundamental Dilators (FD). They interact with other FDs through the metric waves they generate. So, HU immediately recovers the particle-wave dualism.

In addition, HU imposes the Quantum Lagrangian Principle (QLP). QLP states that FDs will move in 4D tangentially to positions where they don't do any work. FDs place themselves where they dilate space in phase with the local dilaton field.

5. HU Replaces Particle-Wave Dualism with the Quantum Trinity

The Quantum Trinity is the recasting of matter as shapeshifting, spinning-in-4D, deformations of space, the observation that all forces are carried by the generated metric waves, and the imposition of the Quantum Lagrangian Principle.

De Broglie waves are mapped to hypersuperficial metric waves, imprinted directly onto the IDL (Inner Dilaton Layer), the dilation layer where all particles surf.

Notice that HU showed that Newton's Laws of Dynamics are equivalent to surfing in the IDL in a 4D Spatial Manifold.

Appendix F: HU Explains the Great Attractor with Epoch-Dependent G

Not all epoch-dependence Gravity models can explain the Great Attractor. The reason is that only at very early times were the tiny density fluctuations close enough to generate the highest accelerations.

In other words, for the Great Attractor to be simply explained by the same tiny density fluctuations seen in the Cosmic Microwave Background, Gravity would have to be very strong, and we would have to be in the vicinity of a bubble of higher density.

HU modeled the low-frequency fluctuations (larger-structure universe) as frozen Neutronium Acoustic Oscillations. Those were modeled using Hyperspherical Harmonics. HU used the SMICA CMB observation by the Planck Satellite and reproduced it using Hyperspherical Harmonics. The CMB appears as density fluctuations on the surface of a sphere embedded in the hyperspherical hypersurface. This means that hyperspherical harmonics are not a full set capable of representing any density profile in the sphere. Instead, only on a given spot in the hypersphere is that possible. That is Earth's location within the hyperspherical universe.

Once the location was found, the hyperspherical harmonic spectral components were determined. With them, one can calculate the density anywhere within the hypersphere, including within the volume of our Observable Universe.

In HU, the Surface of Last Scattering took place when the universe was 11.1 million years old (4D radius of 11.1 million light-years). I considered that the Milky Way and other neighboring galaxies were on the edge of a circular bubble of higher density and integrated the equations of motion as the universe expanded. Notice that I am not considering that space stretches.

I varied the radius of the bubble while keeping a density difference of 1 part in 100,000, as seen in the CMB. That was enough to reproduce a current velocity of 1000 km/s within the range of the observed velocity field.

This is consistent with the density profile at the shortest distances in our 3D galaxy density map:

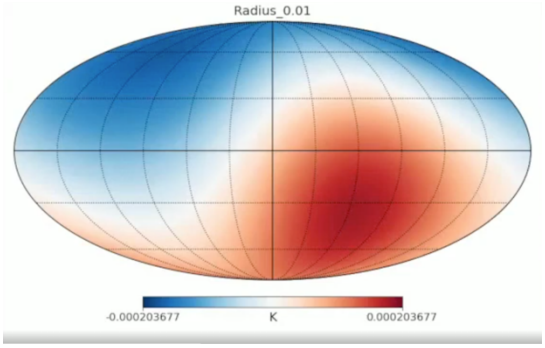

Figure 10. This shows that we are on the edge of a density bubble and that the Great Attractor is predicted with HU's epoch-dependent G.

Here is the full 3D Galaxy Density Map:

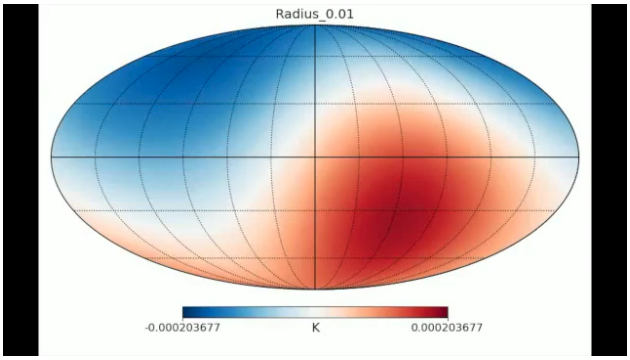

Figure 11. Galaxy density map extracted from Hyperspherical Harmonics Spectral Decomposition of the Cosmic Microwave Background. [13]

There is no other physical explanation consistent with observations, and this is the simplest and strongest evidence of epoch-dependent G.

Appendix G: Epoch-Dependent G and Astrophysics

HU modeled the M33 galaxy evolution across time, showing the effect of stronger G in the past.

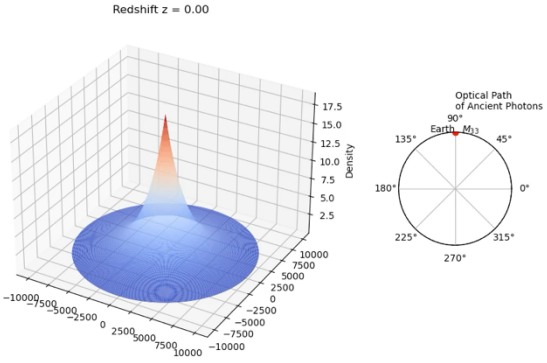

Figure 12. This video shows the M33 galaxy shrinking under the effect of stronger Gravitation at larger redshifts. [14]

This is consistent with the Tolman Surface Brightness Test for Cosmological Theories.

Preliminary Results for HU's Solution to the Early Galaxy Formation Conundrum

These results are preliminary due to computational constraints during calculation.

HU also modeled the Galaxy Formation Process under epoch-dependent G:

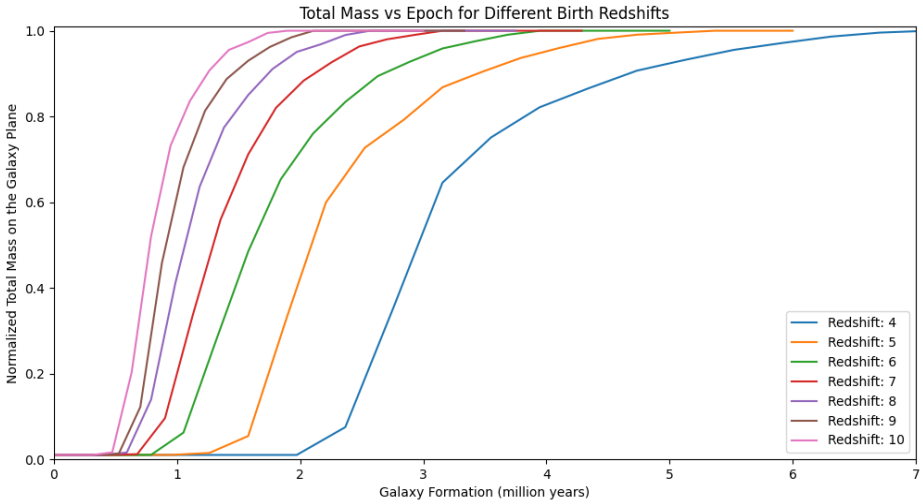

Figure 13. This figure shows the accumulation of mass on the galaxy plane. Galaxies start as tall spinning gas clouds that quickly flatten under their own gravitation. This is consistent with the Cigar-like Galaxies observed by JWST. Angular momentum is conserved. So, the rotation curve for the spinning gas is maintained when stars are formed.

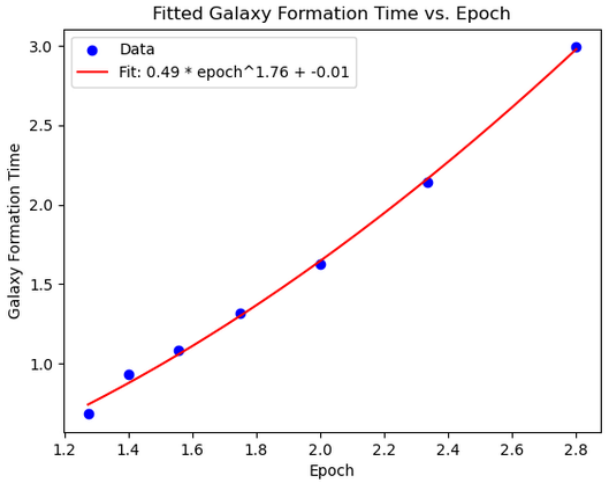

Figure 14. Here, we show the galaxy formation times for different initial starting epochs. All times and epochs in billion years. This means that the earliest galaxies formed in 500 million years.

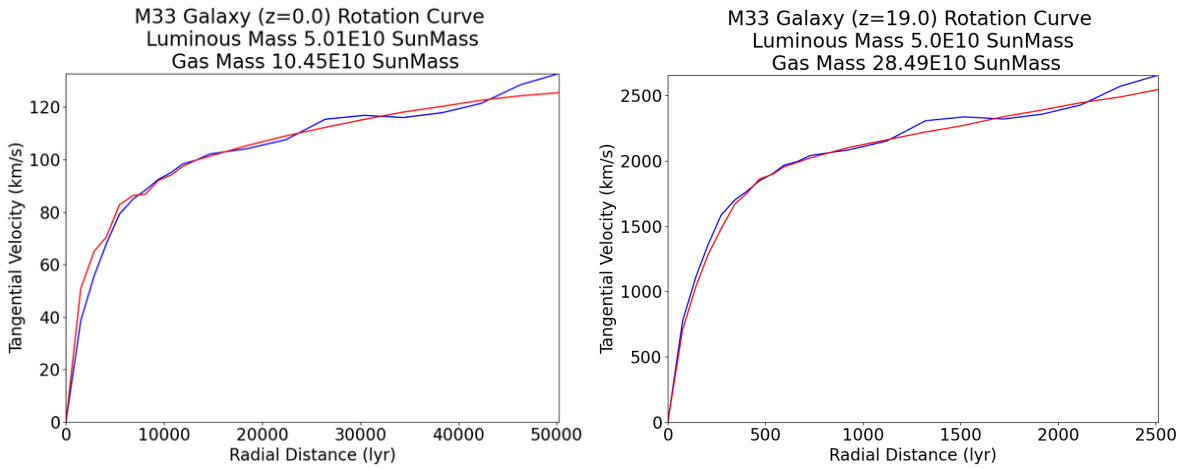

Figure 15. Here, we have M33 at two distinct epochs corresponding to z=0.0 and z=19.0. Notice that the farther M33 senses a 20-fold increase in Gravitation. This reduces the radius by 20-fold and increases velocity by the same amount to conserve angular momentum.

Appendix H: Laws of Nature and General Relativity Tests

1. HOW MATTER INTERACTS

At this point, it becomes clear that Lorentz-Law and variations are incorrect. Because of that, our understanding of how plasma interacts within magnetic confinement, or how neutral matter interacts within spinning Black Holes, is lacking.

The comprehensive force is the sum of the Coulombic/Newton, Lienard-Wichiet, Perihelion Precession, and Biot-Savart forces:

$$\vec{F}_{EM}\left(v_1,v_2\right)=-\vec{F}_{EM}\left(0,0\right)+\vec{F}_{EM}\left(v_1,0\right)+\vec{F}_{EM}\left(0,v_2\right)+\vec{F}_{EM}\left(v_1,v_2\right)=$$

$$-\frac{q_1 q_2}{4\pi\varepsilon_0}\frac{\vec{R}_0}{{R_0}^3} \qquad \#\ Coulomb$$

$$\frac{\left(1-\frac{{v_1}^2}{c^2}\right)}{\left(\left(\gamma_{v2}-1\right)\left(\frac{\dot{r}}{v_2}\right)^2+1\right)}\frac{q_1\cdot q_2}{4\pi\varepsilon_0}\frac{\hat{r}_2}{{R_0}^2}+ \qquad \#\ Lienard-Wichiet$$

$$+\frac{\left(1-\frac{{v_1}^2}{c^2}\right)^{\frac{3}{2}}}{\left(\left(\gamma_{v1}-1\right)\left(\frac{\dot{r}}{v_1}\right)^2+1\right)}\frac{q_1\cdot q_2}{4\pi\varepsilon_0}\frac{\hat{r}_2}{{P_2}^2}+ \qquad \#\ Mercury\ Precession$$

$$\frac{\mu_0}{4\pi}\frac{\vec{J}_1 X\left(\vec{J}_2 X\ \vec{r}_2\right)}{{P_2}^3}HU_{Factor} \qquad \#\ Biot-Savart \qquad (64)$$

Each component corresponds to a given inertial frame option and the physical process studied.

For Gravitation, we have this comprehensive law:

$$\vec{F}_G\left(v_1,v_2\right)=-\vec{F}_G\left(0,0\right)+\vec{F}_G\left(v_1,0\right)+\vec{F}_G\left(0,v_2\right)+\vec{F}_G\left(v_1,v_2\right)=$$

$$-Gm_1m_2\frac{\vec{R}_0}{{R_0}^3} \qquad \#\ Coulomb$$

$$\frac{\left(1-\frac{{v_1}^2}{c^2}\right)}{\left(\left(\gamma_{v2}-1\right)\left(\frac{\dot{r}}{v_2}\right)^2+1\right)}Gm_1m_2\frac{\hat{r}_2}{{R_0}^2}+ \qquad \#\ Lienard-Wichiet$$

$$+\frac{\left(1-\frac{{v_1}^2}{c^2}\right)^{\frac{3}{2}}}{\left(\left(\gamma_{v1}-1\right)\left(\frac{\dot{r}}{v_1}\right)^2+1\right)}Gm_1m_2\frac{\hat{r}_2}{{P_2}^2}+ \qquad \#\ Mercury\ Precession$$

$$\frac{G}{c^2}\frac{\vec{J}_1X\left(\vec{J}_2X\ \ \vec{r}_2\right)}{{P_2}^3}HU_{Factor} \qquad \#\ Biot-Savart$$

$$with\ G=\left(1+z\right)G_0 \qquad (65)$$

and

$$HU_{Factor}\left(v_1,v_2\right)=\frac{\left(\gamma_{v2}-1\right)\left(\hat{r}.\hat{V}_2\right)^2+\hat{r}.\hat{r}}{\left(\gamma_{v1}-1\right)\left(\hat{r}.\hat{V}_1\right)^2+\hat{r}.\hat{r}}\frac{{\gamma_{v1}}^3\sqrt{1+\left(\frac{v_1}{c}\right)^2-2\left(\frac{\dot{r}}{c}\right)}}{\left(\left(\gamma_{v2}-1\right)\frac{\left(\vec{r}_2.\hat{V}_2\right)^2}{\vec{r}_2.\vec{r}_2}+1\right)^2} \qquad (66)$$

HU Laws of Nature correct Einstein's General Relativity, Lienard-Wichiet Retarded Potentials, and Biot-Savart (a.k.a. Lorentz) forces.

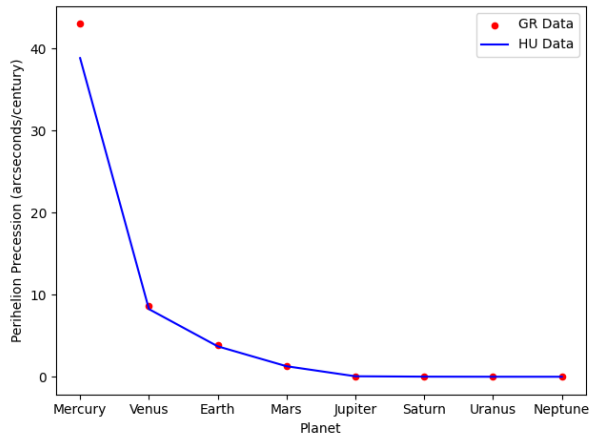

Figure 16. Perihelion Precession Rates for all planets according to HU and General Relativity.

Notice the simplification that HU brings to Physics. Instead of modeling each field as a deformation of Spacetime, HU provides Forces that are described in the Absolute Reference Frame (ARF). ARF is not visible in our 3D Universe, but it is clear in the 4D Spatial Manifold and LEHU. What defines the ARF is

the choice of orientation of the Radial Direction. The vector associated with motion outside our 3D hypersphere has to be the one perpendicular to the hypersphere at each point. Three arbitrary orthogonal vectors inside the hypersphere complete the 4D ARF.

HU's benefits to Physics are irrefutable, as it simplifies it to Forces and Euclidian 4D Spatial Manifold.

Here, we show that when we center the Sun or the center of mass on the Absolute Reference, thus making v2=0, the Gravitational force reduces to:

$$\vec{F}_G\left(v_1,v_2\right)=-\vec{F}_G\left(0,0\right)+\vec{F}_G\left(v_1,0\right)+\vec{F}_G\left(0,v_2\right)+\vec{F}_G\left(v_1,v_2\right)=$$

$$-Gm_1m_2\frac{\vec{R}_0}{{R_0}^3} \qquad \#\ Coulomb$$

$$\frac{\left(1-\frac{{v_1}^2}{c^2}\right)}{\left(\left(\gamma_{v2}-1\right)\left(\frac{\dot{r}}{v_2}\right)^2+1\right)}Gm_1m_2\frac{\hat{r}_2}{{R_0}^2}+ \qquad \#\ Lienard-Wichiet$$

$$+\frac{\left(1-\frac{{v_1}^2}{c^2}\right)^{\frac{3}{2}}}{\left(\left(\gamma_{v1}-1\right)\left(\frac{\dot{r}}{v_1}\right)^2+1\right)}Gm_1m_2\frac{\hat{r}_2}{{P_2}^2}+ \qquad \#\ Mercury\ Precession$$

$$\frac{G}{c^2}\frac{\vec{J}_1X\left(\vec{J}_2X\ \ \vec{r}_2\right)}{{P_2}^3}HU_{Factor} \qquad \#\ Biot-Savart$$

$$with\ G=\left(1+z\right)G_0$$

(67)

Below, you can see HU's Predictions for all planets' Perihelion Precession Rates. Setting v_2=0

$$HU_{Factor}\left(v_1,v_2\right)=\frac{\left(\gamma_{v2}-1\right)\left(\hat{r}.\hat{V}_2\right)^2+\hat{r}.\hat{r}}{\left(\gamma_{v1}-1\right)\left(\hat{r}.\hat{V}_1\right)^2+\hat{r}.\hat{r}}\frac{{\gamma_{v1}}^3\sqrt{1+\left(\frac{v_1}{c}\right)^2-2\left(\frac{\dot{r}}{c}\right)}}{\left(\left(\gamma_{v2}-1\right)\frac{\left(\vec{r}_2.\hat{V}_2\right)^2}{\vec{r}_2.\vec{r}_2}+1\right)^2} \qquad (68)$$

Since

$$\hat{r}=\frac{\vec{r}_2}{R_0}=\frac{\vec{R}_0-\vec{V}_1\frac{R_0}{c}}{R_0}=\hat{R}_0-\frac{\vec{V}_1}{c} \qquad (69)$$

$$P_2=\left|\hat{r}\right|=\sqrt{1+\left(\frac{v_1}{c}\right)^2-2\left(\frac{\dot{r}}{c}\right)} \qquad (70)$$

HU also predicts the correct Gravitational Time Dilation, SR Time Dilation, Binary Pulsar Gravitational Energy Emission, and LIGO Signals and does all that without requiring Space Stretching, Dark Matter, Dark Energy, Higgs Mechanism for Inertia, False Vacuum Decay, Inflaton Field, Inflaton Particles, Inflation, Massless Particles, and the Annihilation of an Equal Universe Mass of Antimatter.

HU also shows that simple idiosyncratic radial exponential mass distributions are enough to explain the Spiral Galaxy Rotation Curve Conundrum without the need for any Dark Matter.

The Universe was uniform (1 part in 100,000 density fluctuation). It is obvious that that uniformity remained. The difference is that in higher-density regions, there are more galaxies and less mass contained in the gas clouds, while in lower-density regions, the galaxy density is lower, and there is more gas.

What many Dark Matter surveys have detected intergalactic might be just gas. That is the logical conclusion from observing the Cosmic Microwave Background. From the homogeneous plasma distribution, one can only create a homogeneous universe.

References

1. Williams, J. G., Turyshev, S. G., & Boggs, D. H. (2004). Progress in lunar laser ranging tests of relativistic gravity. Physical Review Letters, 93(26 I). https://doi.org/10.1103/PhysRevLett.93.261101
2. Williams, J. ~G., Newhall, X. ~X., & Dickey, J. ~O. (1987). Lunar Science From Lunar Laser Ranging. Lunar and Planetary Science Conference, 116.
3. Sahni, V., & Shtanov, Y. (2014). Can a variable gravitational constant resolve the faint young Sun paradox? International Journal of Modern Physics D, 23(12). DOI: 10.1142/S0218271814420188, arXiv:1405.4369.
4. Mould, J., & Uddin, S. A. (2014). Constraining a possible variation of G with type Ia supernovae. Publications of the Astronomical Society of Australia, 31(1), 1–15. DOI: 10.1017/pasa.2014.9.
5. Arnett, D. (1980). Analytic Solution for Light Curves of Supernovae of Type II. The Astrophysical Journal, 237, 541–549.
6. Pereira, M. (2024). *The Hypergeometrical Universe Theory*. https://doi.org/10.2139/SSRN.5012064
7. Pereira, M. (2024). *Hu -The Big Pop Cosmogenesis Equation of State*. https://doi.org/10.2139/SSRN.5012159
8. Pereira, M. (2024). *ny2292000/HU_Papers: Repository with HU Papers*. https://github.com/ny2292000/HU_Papers
9. Pereira, M. (2024). *ny2292000/HU_Galaxy_docker* https://github.com/ny2292000/HU_Galaxy_docker
10. Pereira, M. (2024). *ny2292000/HU_GalaxyPackage*. https://github.com/ny2292000/HU_GalaxyPackage
11. Pereira, M. (2024). *Pereira's Github CMB Repository*. https://github.com/ny2292000/CMB_HU
12. Brodsley, L., Frank, C., & Steeds, J. W. (1986). Prince Rupert's Drops. *Notes and Records of the Royal Society of London*, *41*(1), 1–26. https://doi.org/10.1098/rsnr.1986.0001
13. HU's Galaxy Density Map Prediction. https://youtu.be/MLqkbCAzcJ
14. HU's M33 Galaxy Evolution Prediction. https://youtu.be/A3buediDHUU